Scientia Iranica B (2016) 23(4), 1787–1799

Sharif University of Technology
Scientia Iranica
Transactions B: Mechanical Engineering
www.scientiairanica.com

Finite element formulations for free vibration analysis of isotropic and orthotropic plates using two-variable refined plate theory

J. Rouzegar* **and R. Abdoli Sharifpoor**

Department of Mechanical and Aerospace Engineering, Shiraz University of Technology, Shiraz, P.O. Box 71555-313, Iran.

Received 1 January 2015; received in revised form 7 July 2015; accepted 15 September 2015

KEYWORDS
Finite element method;
Free vibration;
Rectangular plate element;
Two-variable refined plate theory.

Abstract. In this paper, a finite element formulation based on two-variable refined plate theory is developed for free vibration analysis of isotropic and orthotropic plates. The two-variable refined plate theory, which can be used for both thin and thick plates, predicts parabolic variation of transverse shear stresses across the plate thickness, satisfies the zero traction condition on the plate surfaces, and does not need the shear correction factor. After constructing weak-form equations using the Hamilton principle for vibration formulation, a new 4-node rectangular plate element with six degrees of freedom at each node is introduced for discretization of the domain. The natural frequencies of isotropic plates with different boundary conditions and the fundamental natural frequencies of levy-type orthotropic plates are obtained. Comparison of results with exact solutions and other common plate theories shows that besides simplicity of the presented finite element formulations, they present accurate and efficient results. Also, the effects of orthotropy ratio, side-to-thickness ratio, and types of boundary conditions on the natural frequencies are studied.

1. Introduction

Classical Plate Theory (CPT) is the simplest plate theory that gives good results for bending analysis of thin plates, but it does not take transverse shear deformation effects into account. The effect of shear deformation is important in bending analysis of thick plates and also for thin plates vibrating at higher modes; thus, numerous researchers have attempted to refine the CPT. Reissner proposed First-order Shear Deformation Theory (FSDT) based on stress approach [1] and another form of FSDT was proposed by Mindlin [2] based on displacement approach. The FSDT predicts the constant transverse shear stress along the plate thickness and hence the zero-stress conditions on free surfaces cannot be satisfied. Also, this theory needs the shear correction factor in formulation. To resolve these deficiencies, Higher-order Shear Deformation Theories (HSDTs) were developed. Second-order shear deformation theory of Whitney and Sun [3], third-order shear deformation theory of Hanna and Leissa [4], Reddy [5], Bhimaraddi and Stevens [6], Kant [7], and Lo et al. [8] are some famous HSDTs.

Recently, some new higher-order shear deformation theories such as trigonometric shear deformation theory [9], hyperbolic shear deformation theory [10], and two-variable refined plate theory [11] have been developed. The two-variable plate theory (RPT) is a simple and efficient theory that contains only two unknown variables which are bending and shear components of transverse displacement. This theory satisfies the zero-stress conditions on free surfaces and does not need the shear correction factor in formulation. It was introduced by Shimpi [11] for isotropic plates and then extended to orthotropic plates by Shimpi

*. *Corresponding author. Tel./Fax: +98 71 37264102*
E-mail address: rouzegar@sutech.ac.ir (J. Rouzegar)

and Patel [12] and Thai and Kim [13]. The analysis of laminated composite plates was done by Kim et al. [14] and the vibration and buckling analyses of plates were performed by Shimpi and Patel [15] and Kim et al. [16], respectively. Levy-type solution for buckling analysis of orthotropic plates was studied by Thai and Kim [17]. Considering non-local effects, the buckling behavior of isotropic nano-plates was studied by Narender [18]. Free vibration of nano-plates was performed by Malekzadeh and Shojaee [19] using differential quadrature method for solution of the governing equations.

Previous researchers have adopted the two-variable plate theory and presented analytical solutions for some plate problems with specific geometry, loading, and boundary conditions. In practice, it is too difficult to solve many engineering problems by common analytical methods. Using numerical approaches, the complicated problems could be simulated in an approximate manner. Bhat [20] obtained natural frequencies by employing a set of characteristic orthogonal polynomials in the Rayleigh-Ritz method. This method yields superior results for lower modes, particularly when plates have some of the edges free. Misra [21] implemented the multi-quadratic radial basis function for free vibration analysis of isotropic plate. This method gives relatively good results, but its implementation is not simple. Semnani et al. [22] applied two-dimensional differential transfer method for investigating free vibration behavior of variable thickness plates with different boundary conditions. Liew et al. [23] adopted the first-order shear deformation theory in the moving least squares differential quadrature method for predicting the free vibration behavior of moderately thick symmetrically laminated composite plates.

One of the popular and interesting numerical techniques is finite element method. Finite element analysis became quick, precise, and popular by the advancements in computer sciences. Recently, a finite element formulation based on two-variable refined plate theory was developed for bending analysis of thin and thick orthotropic plates [24]. In this study, a new Finite Element formulation based on two-variable Refined Plate Theory (FE-RPT formulation) has been developed for free vibration analysis of thin and thick isotropic and orthotropic plates. A new 4-node rectangular plate element with six degrees of freedom at each node has been introduced. Besides accuracy of the developed formulation, it is very simple to implement in comparison to other shear deformation finite element methods. This formulation can be used for both thin and thick plates and is free from shear locking in contrast to first-shear deformation finite element formulation. This formulation predicts parabolic transverse shear stresses across the plate thickness and satisfies the zero-stress conditions on free surfaces. Accuracy and efficiency of the presented formulation have been proved by solving some benchmark problems in the literature.

2. Theory of problem

2.1. Two-variable refined plate theory

The two-variable refined plate theory is constructed based on the following assumptions:

1. The displacements (u in x-direction, v in y-direction, and w in z-direction) are small relative to the plate thickness. Thus, the strain-displacement relations can be expressed as follows:

$$\begin{cases} \varepsilon_x = \frac{\partial u}{\partial x}, & \gamma_{xy} = \frac{\partial v}{\partial x} + \frac{\partial u}{\partial y}, \\ \varepsilon_y = \frac{\partial v}{\partial y}, & \gamma_{yz} = \frac{\partial w}{\partial y} + \frac{\partial v}{\partial z}, \\ \varepsilon_z = \frac{\partial w}{\partial z}, & \gamma_{zx} = \frac{\partial w}{\partial x} + \frac{\partial u}{\partial z}, \end{cases} \tag{1}$$

   where ε_x, ε_y, and ε_z are normal strains in x, y, and z directions and γ_{xy}, γ_{yz}, and γ_{zx} are shear strains in z, x, and y planes, respectively.

2. The displacement field (u in x-direction, v in y-direction, and w in z-direction) consists of bending and shear components:

$$w(x, y, t) = w_b(x, y, t) + w_s(x, y, t),$$

$$u = u_b + u_s, \qquad v = v_b + v_s. \tag{2}$$

   The bending components of in-plane displacement play the same roles as those of u and v in classical plate theory. Thus, we can write:

$$u_b = -z\frac{\partial w_b}{\partial x}, \qquad v_b = -z\frac{\partial w_b}{\partial y}. \tag{3}$$

3. The stress normal to the middle plane, σ_z, is small compared with other stress components and may be neglected in the stress-strain relations. Consequently, the stress-strain relations for an orthotropic plate can be written as:

$$\begin{cases} \sigma_x = \frac{E_1}{1-\mu_{12}\mu_{21}}(\varepsilon_x + \mu_{12}\varepsilon_y) \\ \sigma_y = \frac{E_2}{1-\mu_{12}\mu_{21}}(\varepsilon_y + \mu_{21}\varepsilon_x) \\ \sigma_z = 0 \qquad \tau_{xy} = G_{12}\gamma_{xy} \qquad \tau_{yz} = G_{23}\gamma_{yz} \\ \qquad\qquad \tau_{zx} = G_{31}\gamma_{zx} \end{cases} \tag{4}$$

   where σ_x, σ_y, and σ_z are normal stresses in x, y, and z directions and τ_{xy}, τ_{yz}, and τ_{zx} are shear stresses. E_1 and E_2 are elastic moduli; G_{12}, G_{23}, and G_{31} are shear moduli; and μ_{12}, and μ_{21} are Poisson's ratios.

4. Shear components of in-plane displacement are considered as the following functions:

$$u_s = h\left[\frac{1}{4}\left(\frac{z}{h}\right) - \frac{5}{3}\left(\frac{z}{h}\right)^3\right]\frac{\partial w_s}{\partial x},$$

$$v_s = h\left[\frac{1}{4}\left(\frac{z}{h}\right) - \frac{5}{3}\left(\frac{z}{h}\right)^3\right]\frac{\partial w_s}{\partial y}. \quad (5)$$

Based on the above assumptions, the displacements can be calculated as:

$$u(x,y,z) = -z\frac{\partial w_b}{\partial x} + h\left[\frac{1}{4}\left(\frac{z}{h}\right) - \frac{5}{3}\left(\frac{z}{h}\right)^3\right]\frac{\partial w_s}{\partial x}, \quad (6)$$

$$v(x,y,z) = -z\frac{\partial w_b}{\partial y} + h\left[\frac{1}{4}\left(\frac{z}{h}\right) - \frac{5}{3}\left(\frac{z}{h}\right)^3\right]\frac{\partial w_s}{\partial y}, \quad (7)$$

$$w(x,y,t) = w_b(x,y,t) + w_s(x,y,t). \quad (8)$$

The strain field is obtained by substituting Eqs. (6)-(8) in Eq. (1):

$$\varepsilon_x = -z\frac{\partial^2 w_b}{\partial x^2} + h\left[\frac{1}{4}\left(\frac{z}{h}\right) - \frac{5}{3}\left(\frac{z}{h}\right)^3\right]\frac{\partial^2 w_s}{\partial x^2}, \quad (9)$$

$$\varepsilon_y = -z\frac{\partial^2 w_b}{\partial y^2} + h\left[\frac{1}{4}\left(\frac{z}{h}\right) - \frac{5}{3}\left(\frac{z}{h}\right)^3\right]\frac{\partial^2 w_s}{\partial y^2}, \quad (10)$$

$$\varepsilon_z = 0, \quad (11)$$

$$\gamma_{xy} = -2z\frac{\partial^2 w_b}{\partial x\partial y} + 2h\left[\frac{1}{4}\left(\frac{z}{h}\right) - \frac{5}{3}\left(\frac{z}{h}\right)^3\right]\frac{\partial^2 w_s}{\partial x\partial y}, \quad (12)$$

$$\gamma_{yz} = \left[\frac{5}{4} - 5\left(\frac{z}{h}\right)^2\right]\frac{\partial w_s}{\partial y}, \quad (13)$$

$$\gamma_{xz} = \left[\frac{5}{4} - 5\left(\frac{z}{h}\right)^2\right]\frac{\partial w_s}{\partial x}. \quad (14)$$

Substituting strains in constitutive Eqs. (4), the expressions for stresses can be obtained as the following equations:

$$\begin{Bmatrix}\sigma_x\\ \sigma_y\\ \tau_{xy}\\ \tau_{yz}\\ \tau_{zx}\end{Bmatrix} = \begin{bmatrix}Q_{11} & Q_{12} & 0 & 0 & 0\\ Q_{12} & Q_{22} & 0 & 0 & 0\\ 0 & 0 & Q_{66} & 0 & 0\\ 0 & 0 & 0 & Q_{44} & 0\\ 0 & 0 & 0 & 0 & Q_{55}\end{bmatrix}\begin{Bmatrix}\varepsilon_x\\ \varepsilon_y\\ \gamma_{xy}\\ \gamma_{yz}\\ \gamma_{zx}\end{Bmatrix}, \quad (15)$$

where:

$$\begin{cases} Q_{11} = \frac{E_1}{1-\mu_{12}\mu_{21}}, \qquad Q_{12} = \frac{\mu_{12}E_2}{1-\mu_{12}\mu_{21}} = \frac{\mu_{21}E_2}{1-\mu_{12}\mu_{21}},\\ Q_{22} = \frac{E_2}{1-\mu_{12}\mu_{21}},\\ \\ Q_{44} = G_{23}, \qquad Q_{55} = G_{31}, \qquad Q_{66} = G_{12}\end{cases} \quad (16)$$

2.2. The governing equations of free vibration

The governing equations and boundary conditions of time-dependent problems can be obtained using Hamilton's principle:

$$0 = \int_{t_1}^{t_2}\delta(T-U)dt. \quad (17)$$

The kinetic energy and total potential energy of a rectangular plate (of length a, width b, and thickness h) can be written as Eqs. (18) and (19), respectively:

$$T = \int_{z=-h/2}^{z=h/2}\int_{y=0}^{y=b}\int_{x=0}^{x=a}\frac{1}{2}\rho\left[\left(\frac{\partial u}{\partial t}\right)^2 + \left(\frac{\partial v}{\partial t}\right)^2 + \left(\frac{\partial w}{\partial t}\right)^2\right]dxdydz, \quad (18)$$

$$U = \int_{z=-h/2}^{z=h/2}\int_{y=0}^{y=b}\int_{x=0}^{x=a}\frac{1}{2}[\sigma_x\varepsilon_x + \sigma_y\varepsilon_y + \tau_{xy}\gamma_{xy} + \tau_{yz}\gamma_{yz} + \tau_{zx}\gamma_{zx}]dxdydz, \quad (19)$$

where ρ is mass density. By substituting Eqs. (18) and (19) into (17) and taking the independent variations of w_b and w_s into account, the governing equations are obtained as Eqs. (20) and (21):

$$D_{11}\frac{\partial^4 w_b}{\partial x^4} + 2(D_{12}+2D_{66})\frac{\partial^4 w_b}{\partial x^2\partial y^2} + D_{22}\frac{\partial^4 w_b}{\partial x^4} - \frac{\rho h^3}{12}\frac{\partial^2}{\partial t^2}(\nabla^2 w_b) + \rho h\left(\frac{\partial^2 w_b}{\partial t^2} + \frac{\partial^2 w_s}{\partial t^2}\right) = 0, \quad (20)$$

$$\frac{1}{84}\left[D_{11}\frac{\partial^4 w_s}{\partial x^4} + 2(D_{12}+2D_{66})\frac{\partial^4 w_s}{\partial x^2\partial y^2} + D_{22}\frac{\partial^4 w_s}{\partial x^4}\right] - \left[A_{55}\frac{\partial^2 w_s}{\partial x^2} + A_{44}\frac{\partial^2 w_s}{\partial y^2}\right] - \frac{\rho h^3}{1008}\frac{\partial^2}{\partial t^2}(\nabla^2 w_s) + \rho h\left(\frac{\partial^2 w_b}{\partial t^2} + \frac{\partial^2 w_s}{\partial t^2}\right) = 0, \quad (21)$$

where D_{11}, D_{22}, D_{12}, D_{66}, A_{44}, and A_{55} are plate-material stiffness defined in Eq. (22):

$$\begin{cases} D_{11} = \frac{Q_{11}h^3}{12}, \qquad D_{22} = \frac{Q_{22}h^3}{12}, \qquad D_{12} = \frac{Q_{12}h^3}{12},\\ \qquad\qquad D_{66} = \frac{Q_{66}h^3}{12},\\ \\ A_{44} = \frac{5Q_{44}h}{6}, \qquad A_{55} = \frac{5Q_{55}h}{6}.\end{cases} \quad (22)$$

As can be seen, the governing equations are given by two fourth-order differential equations that are coupled for dynamic problems and uncoupled for static problems. Different possible boundary conditions were discussed in [12].

2.3. Finite element formulation of free vibration

Based on two-variable refined plate theory, the weak-form equations for free vibration analysis are obtained by substituting kinetic and potential energies in function of displacements into Hamilton's principle, integrating them across the plate thickness, and then using the calculus of variation technique:

$$\begin{aligned}
0 =& \frac{\rho h^3}{12}\int_{\Omega^e}\left[\left(\frac{\partial^3 w_b}{\partial x\partial t^2}\frac{\partial \delta w_b}{\partial x}+\frac{\partial^3 w_b}{\partial y\partial t^2}\frac{\partial \delta w_b}{\partial y}\right)\right]dxdy \\
&+\frac{\rho h^3}{1008}\int_{\Omega^e}\left[\left(\frac{\partial^3 w_s}{\partial x\partial t^2}\frac{\partial \delta w_s}{\partial x}+\frac{\partial^3 w_s}{\partial y\partial t^2}\frac{\partial \delta w_s}{\partial y}\right)\right]dxdy \\
&+\int_{\Omega_e}\left[\left(D_{11}\frac{\partial^2 w_b}{\partial x^2}+D_{12}\frac{\partial^2 w_b}{\partial y^2}\right)\frac{\partial^2 \delta w_b}{\partial x^2}\right. \\
&+\left(D_{12}\frac{\partial^2 w_b}{\partial x^2}+D_{22}\frac{\partial^2 w_b}{\partial y^2}\right)\frac{\partial^2 \delta w_b}{\partial y^2} \\
&\left.+4D_{66}\frac{\partial^2 w_b}{\partial x\partial y}\frac{\partial^2 \delta w_b}{\partial x\partial y}\right]dxdy \\
&+\int_{\Omega_e}\left[\frac{1}{84}\left[\left(D_{11}\frac{\partial^2 w_s}{\partial x^2}+D_{12}\frac{\partial^2 w_s}{\partial y^2}\right)\frac{\partial^2 \delta w_s}{\partial x^2}\right.\right. \\
&+\left(D_{12}\frac{\partial^2 w_s}{\partial x^2}+D_{22}\frac{\partial^2 w_s}{\partial y^2}\right)\frac{\partial^2 \delta w_s}{\partial y^2} \\
&\left.+4D_{66}\frac{\partial^2 w_s}{\partial x\partial y}\frac{\partial^2 \delta w_s}{\partial x\partial y}\right]+A_{44}\frac{\partial w_s}{\partial x}\frac{\partial \delta w_s}{\partial x} \\
&\left.+A_{55}\frac{\partial w_s}{\partial y}\frac{\partial \delta w_s}{\partial y}\right]dxdy \\
&+\rho h\int_{\Omega^e}\left[\frac{\partial}{\partial t}(\delta w_b+\delta w_s)\left(\frac{\partial w_b}{\partial t}+\frac{\partial w_s}{\partial t}\right)\right]dxdy. \qquad (23)
\end{aligned}$$

Eq. (23) can be rewritten in the following vector form:

$$\begin{aligned}
&\int_{\Omega^e}\left\{\left[I_0(\delta w_b)^T\ddot{w}_b+I_2(D_1\delta w_b)^T(D_1\ddot{w}_b)\right]\right. \\
&\left.+\left[I_0(\delta w_s)^T\ddot{w}_s+\frac{I_2}{84}(D_1\delta w_s)^T(D_1\ddot{w}_s)\right]\right\}dxdy \\
&+\int_{\Omega^e}\left\{I_0(\delta w_s)^T\ddot{w}_b+I_0(\delta w_b)^T\ddot{w}_s\right\}dxdy \\
&+\int_{\Omega^e}\left\{[(D_2\delta w_b)^T D(D_2 w_b)]\right. \\
&+\left[\frac{1}{84}(D_2\delta w_s)^T D(D_2 w_s)\right. \\
&\left.\left.+(D_1\delta w_s)^T A(D_1 w_s)\right]\right\}dxdy=0, \qquad (24)
\end{aligned}$$

where I_0, I_2, A, D, D_1, and D_2 are defined as:

$$\begin{aligned}
&I_0=\rho h, \qquad I_2=\frac{\rho h^3}{12}, \qquad A=\begin{bmatrix}A_{44}&0\\0&A_{55}\end{bmatrix}, \\
&D=\begin{bmatrix}D_{11}&D_{12}&0\\D_{12}&D_{22}&0\\0&0&D_{66}\end{bmatrix}, \qquad D_1=\begin{Bmatrix}\frac{\partial}{\partial x}\\\frac{\partial}{\partial y}\end{Bmatrix}, \\
&D_2=\begin{Bmatrix}\frac{\partial^2}{\partial x^2}\\\frac{\partial^2}{\partial y^2}\\2\frac{\partial^2}{\partial x\partial y}\end{Bmatrix}. \qquad (25)
\end{aligned}$$

The bending and shear transverse displacement fields can be determined by interpolating the nodal Degrees Of Freedom (DOFs) over the domain of elements:

$$\begin{aligned}
w_b(x,y)&=\sum_{j=1}^{n}\Delta_j^b\varphi_j(x,y)=N^T\Delta_b, \\
w_s(x,y)&=\sum_{j=1}^{n}\Delta_j^s\varphi_j(x,y)=N^T\Delta_s, \qquad (26)
\end{aligned}$$

where Δ_b and Δ_s are bending and shear DOF vectors in each element, and φ_j and N are interpolation functions and shape functions, respectively. By substituting Eq. (26) into Eq. (24), the finite element equations for free vibration analysis based on two-variable refined plate theory are obtained:

$$\begin{bmatrix}M^{11}&M^{12}\\M^{12}&M^{22}\end{bmatrix}\begin{Bmatrix}\ddot{\Delta}_b\\\ddot{\Delta}_s\end{Bmatrix}+\begin{bmatrix}K^{11}&0\\0&K^{22}\end{bmatrix}\begin{Bmatrix}\Delta_b\\\Delta_s\end{Bmatrix}=\begin{Bmatrix}0\\0\end{Bmatrix}. \qquad (27)$$

It is obvious that the obtained finite element equations are inertially coupled. The elemental mass, stiffness, and force matrices are defined in the following equations:

$$\begin{aligned}
M^{11}&=\int_{\Omega_e}[I_0NN^T+I_2B_1^TB_1]dxdy, \\
M^{22}&=\int_{\Omega_e}\left[I_0NN^T+\frac{I_2}{84}B_1^TB_1\right]dxdy, \\
M^{12}&=\int_{\Omega_e}[I_0NN^T]dxdy,
\end{aligned}$$

$$K^{11} = \int_{\Omega_e} [B_2^T D B_2] dx dy,$$

$$K^{22} = \int_{\Omega_e} \left[\frac{1}{84} B_2^T D B_2 + B_1^T A B_1 \right] dx dy,$$

$$B_1 = D_1 N^T, \qquad B_2 = D_2 N^T. \tag{28}$$

If the effect of shear deformation is ignored and just bending degrees of freedom are considered, the finite element formulation for classical plate theory will be obtained:

$$M^{11} \ddot{\Delta}_b + K^{11} \Delta_b = 0. \tag{29}$$

2.4. Linear rectangular element

A 4-node rectangular plate element with bending and shear capabilities is utilized for discretization of problems domains. As shown in Figure 1, each node has six degrees of freedom, including bending and shear components of transverse displacement and also their first derivatives with respect to x and y:

$$\text{DOFs}: \left\{ w_b \quad \frac{\partial w_b}{\partial x} \quad \frac{\partial w_b}{\partial y} \quad w_s \quad \frac{\partial w_s}{\partial x} \quad \frac{\partial w_s}{\partial y} \right\}. \tag{30}$$

If the shear and bending nodal DOFs are defined by a_i^b and a_i^s, respectively, and the elemental shear and bending DOFs are defined by a_e^b and a_e^s, we will have:

$$a_e^b = \begin{Bmatrix} a_i^b \\ a_j^b \\ a_k^b \\ a_l^b \end{Bmatrix}, \qquad a_i^b = \begin{Bmatrix} w_b \\ \partial w_b/\partial y \\ -\partial w_b/\partial x \end{Bmatrix},$$

$$a_e^s = \begin{Bmatrix} a_i^s \\ a_j^s \\ a_k^s \\ a_l^s \end{Bmatrix}, \qquad a_i^s = \begin{Bmatrix} w_s \\ \partial w_s/\partial y \\ -\partial w_s/\partial x \end{Bmatrix}. \tag{31}$$

For each pair of bending and shear nodal DOFs a_i^b and a_i^s, the shape functions in terms of normalized coordinates can be defined as follows [25]:

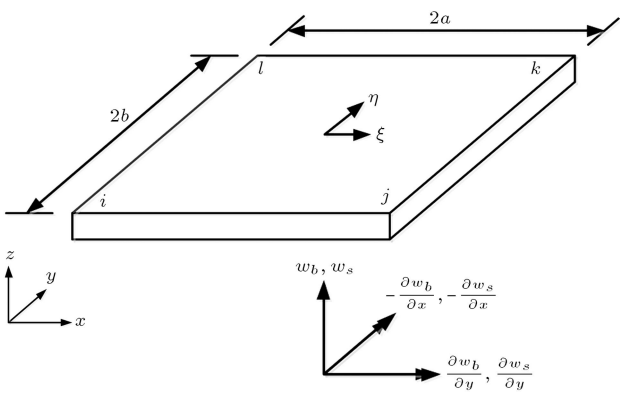

Figure 1. Rectangular plate element.

$$N_i^T = \frac{1}{8}(1+\xi_0)(1+\eta_0) \begin{Bmatrix} (2+\xi_0+\eta_0-\xi^2-\eta^2) \\ b\eta_i(1-\eta^2) \\ -a\xi_i(1-\xi^2) \end{Bmatrix},$$

$$\xi = (x - x_c)/a, \qquad \eta = (y - y_c)/b, \qquad \xi_0 = \xi\xi_i,$$

$$\eta_0 = \eta\eta_i, \tag{32}$$

where $2a$ and $2b$ are the width and length of rectangular element as shown in Figure 1.

3. Results and discussion

Two MATLAB codes, one based on Finite Element formulation of two-variable Refined Plate Theory (shortly FE-RPT) and the other based on Finite Element formulation of Classical Plate Theory (shortly FE-CPT), are prepared for free vibration analysis of isotropic and orthotropic plates and afterwards, some benchmark problems are solved by these codes and the obtained results are compared with the existing analytical solutions of the common plate theories.

3.1. Isotropic plates

In this section, the free vibration of isotropic rectangular plates has been studied. Since the material property is independent of the coordinates, the material properties in Eq. (4) can be given as:

$$E_1 = E_2 = E, \qquad G_{12} = G_{23} = G_{13} = G,$$

$$\mu_{12} = \mu_{21} = \mu. \tag{33}$$

The Poisson ratio is assumed to be 0.3 and the normalized frequency is defined as Eq. (34):

$$\bar{\omega}_{mn} = \omega_{mn} a \sqrt{\rho/G}. \tag{34}$$

Figure 2 shows the convergence study of two vibration modes for a simply supported square plate with $h/a = 0.1$. As seen in this figure, by increasing the number of elements, the results converge to the exact values. Convergence rate of lower vibration mode is faster than that of higher mode. In subsequent problems, 20 elements are considered at each plate edge to insure the convergence of results as shown in Figure 3.

Tables 1 and 2 present the obtained natural frequencies for simply supported isotropic square plate with $h/a = 0.01$ and $h/a = 0.1$. For thin plates, the results of FE-RPT and FE-CPT formulations are very close and both are in good agreement with FSDT results. But in case of thick plate (Table 2), results of FE-RPT are closer to the exact values than those of FE-CPT code. For thin plates, at low-vibration modes,

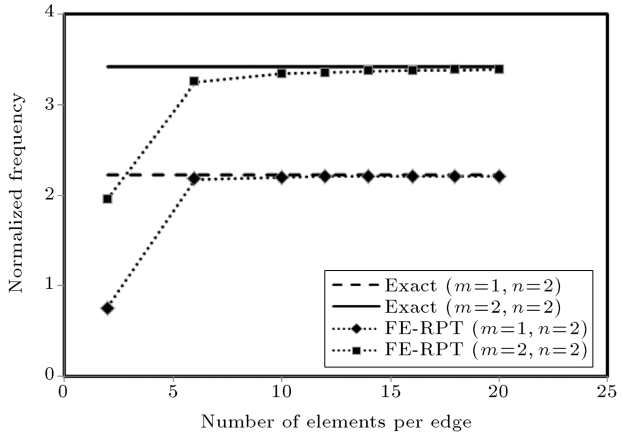

Figure 2. Mesh-independency study for SSSS plate.

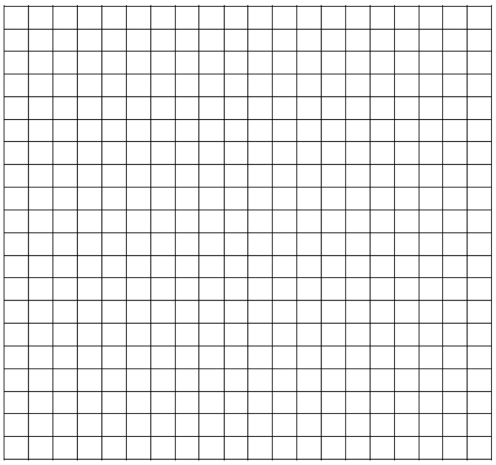

Figure 3. Final mesh of square plate.

Table 1. Comparison of $\bar{\omega}$ for SSSS square plate with $a/h = 100$.

m	n	FSDT [26]	FE-CPT	FE-RPT
1	1	0.0936	0.0962	0.0962
2	1	0.2406	0.2402	0.2401
1	2	0.2406	0.2402	0.2401
2	2	0.3847	0.3831	0.3827
3	1	0.4807	0.4803	0.4796
1	3	0.4807	0.4803	0.4796
3	2	0.6246	0.6212	0.6201
2	3	0.6246	0.6212	0.6201

the results of the present FE-RPT formulation and FE-CPT formulation are identical; but at higher modes, these formulations have some discrepancies, which means that though considering shear deformation effect is important for thick plates, it has significant effect on higher frequency modes of thin plates, too.

Figure 4 illustrates the percentage error of both FE-CPT and FE-RPT formulations in estimation of natural frequencies of a simply supported square plate.

Table 2. Comparison of $\bar{\omega}$ for SSSS square plate with $a/h = 10$.

m	n	Exact [27]	FE-CPT	FE-RPT
1	1	0.932	0.954	0.929
1	2	2.226	2.355	2.215
2	2	3.421	3.712	3.391
1	3	4.171	4.618	4.142
2	3	5.239	5.907	5.178
3	3	6.889	7.996	6.781
2	4	7.511	8.852	7.408
1	5	9.268	10.167	9.389

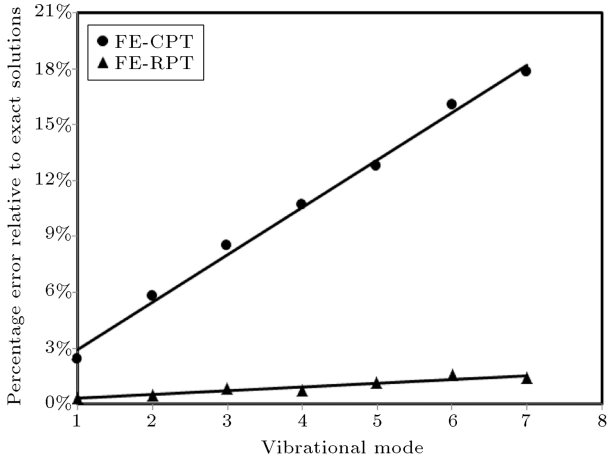

Figure 4. Effect of shear strain on different vibration modes.

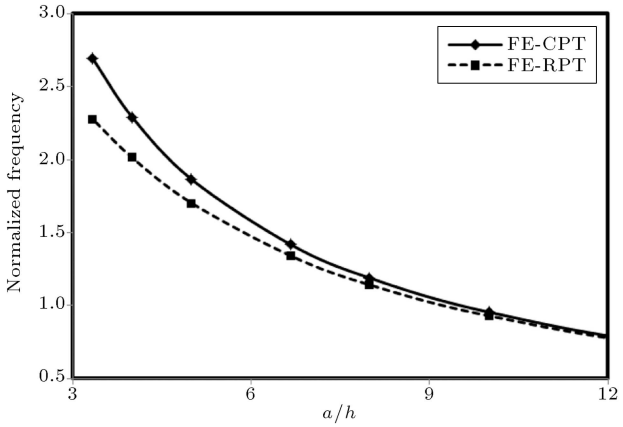

Figure 5. Effect of side-to-thickness ratio on $\bar{\omega}_n$ for FE-RPT and FE-CPT.

The precision of FE-RPT formulation is higher than that of FE-CPT formulation and by increasing the vibration mode, FE-CPT formulation errors increase sharply, but the FE-RPT formulation errors remain nearly constant. It can be concluded that classical plate theory overpredicts all the vibration frequencies for thick plates and higher frequencies for thin plates, as discussed before.

Figure 5 shows the effect of side-to-thickness ratio

on the fundamental natural frequency obtained by both FE-RPT and FE-CPT formulations. For thick plates, results of FE-CPT differ from those of FE-RPT and by decreasing the plate thickness, the results of FE-RPT coincide with those of FE-CPT, which shows that shear locking in the presented formulation does not occur.

It can be concluded that though FE-RPT leads to good results for vibrating of both thin and thick plates in lower and higher modes, FE-CPT gives good results just for vibrating of thin plate in lower modes. Since in FE-RPT formulation, two sets of fourth-order differential equations should be solved, the computational time is nearly twice that of FE-CPT formulation; but in comparison to other higher-order shear deformation theories, the FE-RPT formulation is simple and efficient. It must be noticed that CPT formulation cannot predict shear deformation effects and is completely weak in simulation of thick plates and even in prediction of higher-mode natural frequencies of thin plates.

The natural frequencies for fully clamped square isotropic plate are obtained by FE-CPT and FE-RPT formulations and the results are compared with those of FSDT mesh free method [28] in Tables 3 and 4 for thin and thick plates, respectively. Again, in this case, for thick plates, results of FE-RPT formulation are more accurate than those of FE-CPT formulation. For thin plates, results of FE-CPT and FE-RPT formulations are close at lower modes and they diverge for higher frequencies.

Table 3. Comparison of $\bar{\omega}$ for CCCC square plate with $a/h = 100$.

m	n	FSDT [28]	FE-CPT	FE-RPT
1	1	0.1743	0.175	0.175
2	1	0.3576	0.356	0.356
1	2	0.3576	0.356	0.356
2	2	0.5240	0.523	0.522
3	1	0.6465	0.639	0.638
1	3	0.6505	0.643	0.641
3	2	0.8015	0.796	0.794
2	3	0.8015	0.796	0.794

Table 4. Comparison of $\bar{\omega}$ for CCCC square plate with $a/h = 10$.

m	n	FSDT [28]	FE-CPT	FE-RPT
1	1	1.558	1.734	1.603
2	1	3.018	3.487	3.093
1	2	3.018	3.487	3.093
2	2	4.171	5.054	4.351
3	1	5.121	6.122	5.082
1	3	5.159	6.157	5.159
3	2	6.017	7.537	6.203
2	3	6.017	7.537	6.203

Table 5. Comparison of $\bar{\omega}$ for SCSC square plate with $a/h = 100$.

m	n	FSDT [26]	FE-CPT	FE-RPT
1	1	0.141	0.141	0.141
2	1	0.268	0.266	0.266
1	2	0.337	0.337	0.337
2	2	0.460	0.458	0.457
3	1	0.498	0.496	0.496
1	3	0.628	0.628	0.626
3	2	—	0.677	0.676
2	3	—	0.748	0.746

Table 6. Comparison of $\bar{\omega}$ for SCSC square plate with $a/h = 10$.

m	n	FSDT [26]	FE-CPT	FE-RPT
1	1	1.302	1.397	1.324
2	1	2.398	2.607	2.423
1	2	2.888	3.299	2.957
2	2	3.852	4.431	3.924
3	1	4.237	4.775	4.257
1	3	4.936	6.017	5.040
3	2	—	6.431	5.531
2	3	—	7.095	5.934

The natural frequencies for square plate with two clamped opposite edges and two simply supported edges (SCSC) are computed by the present formulations and the results are compared with those of FSDT [26] in Tables 5 and 6. For thin plate, results of FE-RPT and FE-CPT are in good agreement with those of FSDT. In comparison to FDT, FE-RPT formulation gives more accurate results than FE-CPT for thick plate. It should be noticed that the presented formulation is a higher-order shear deformation theory and the related results must differ from FSDT results.

3.2. Orthotropic Levy-type plates

In this section, an orthotropic square plate, which is simply supported on two opposite edges and has arbitrary boundary conditions along the other edges, is considered. For simplicity, a two-letter notation is used to describe the boundary conditions of the remaining edges as shown in Figure 6. For example, SC shows that one edge is simply supported and the other is clamped.

Material properties of orthotropic plates are considered as follows:

$$G_{12}/E_2 = G_{13}/E_2 = 0.5, \qquad G_{23}/E_2 = 0.2,$$

$$\mu_{12} = 0.25. \tag{35}$$

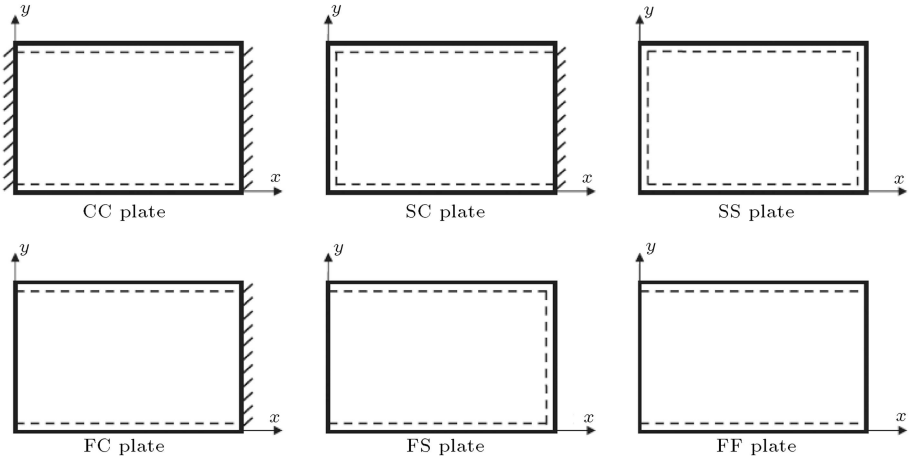

Figure 6. Boundary condition of Levy-type plate [29].

Table 7. Comparison of normalized natural frequency of CC plate.

a/h		E_1/E_2				
		10	**20**	**30**	**40**	**50**
5	FE-RPT	10.8314	11.8276	12.3669	12.7543	13.0698
	FE-CPT	20.4791	28.3771	34.5129	39.7118	43.9438
	RPT [29]	10.8428	11.8374	12.3765	12.7642	13.0803
10	FE-RPT	16.0445	18.9743	20.5200	21.5141	22.2278
	FE-CPT	21.0285	29.1389	35.4397	40.7783	45.4948
	RPT [29]	16.0752	19.0023	20.5455	21.5377	22.2500
20	FE-RPT	19.4384	25.1987	28.9115	31.5873	33.6366
	FE-CPT	21.1728	29.339	35.6831	41.0585	45.8074
	RPT [29]	19.4909	25.2595	28.9746	31.6502	33.6985
50	FE-RPT	20.8991	28.5777	34.3119	38.9887	42.9705
	FE-CPT	21.2137	29.3958	35.7522	41.138	45.8951
	RPT [29]	20.9637	28.6650	34.4146	39.1030	43.0937
100	FE-RPT	21.1392	29.1915	35.3824	40.5744	45.115
	FE-CPT	21.2196	29.4039	35.7621	41.1494	45.9088

The normalized fundamental natural frequency for orthotropic plate is defined as Eq. (36).

$$\bar{\omega} = \omega \frac{a^2}{h} \sqrt{\rho / E_2}. \tag{36}$$

In Table 7, the normalized natural frequencies for CC orthotropic plate with different side-to-thickness (a/h) and orthotropy (E_1/E_2) ratios are compared with analytical RPT solution. For thick plate ($a/h = 5$), the presented FE-RPT formulation has good agreement with analytical RPT solution, but the FE-CPT formulation does not provide proper results. By increasing the side-to-thickness ratio, results of FE-CPT formulation converge to those of FE-RPT, as shown in Figure 7. Also, it is observed that increasing orthotropy ratio causes the normalized natural frequency to increase. The normalized natural frequencies obtained by FE-RPT and FE-CPT formulations for orthotropic plates with SC, SS, FC, FS, and FF edges are compared with the analytical RPT solution in Tables 8-12, respectively, and similar results to those in Table 7 are observed in these tables.

The effects of side-to-thickness ratio on normalized fundamental natural frequency of orthotropic plate

Table 8. Comparison of normalized natural frequency of SC plate.

a/h		E_1/E_2				
		10	**20**	**30**	**40**	**50**
5	FE-RPT	9.5333	10.6768	11.2625	11.6455	11.9307
	FE-CPT	14.6464	19.9556	24.1235	27.6707	30.8122
	RPT [29]	9.5462	10.6878	11.2725	11.6549	11.9399
10	FE-RPT	12.8341	15.7706	17.5131	18.6948	19.5608
	FE-CPT	15.0255	20.4725	24.7487	28.3879	31.6109
	RPT [29]	12.8632	15.8014	17.5431	18.7235	19.5882
20	FE-RPT	14.4516	18.9992	22.2158	24.7015	26.7135
	FE-CPT	15.1249	20.6081	24.9127	28.5760	31.8204
	RPT [29]	14.4921	19.0510	22.2738	24.7632	26.7775
50	FE-RPT	15.0374	20.3574	24.4537	27.8742	30.8475
	FE-CPT	15.1531	20.6466	24.9592	28.6294	31.8798
	RPT [29]	15.0824	20.4197	24.5288	27.9597	30.9416
100	FE-RPT	15.1278	20.5783	24.8359	28.4416	31.6193
	FE-CPT	15.1571	20.6521	24.9658	28.6370	31.8884

Table 9. Comparison of normalized natural frequency of SS plate.

a/h		E_1/E_2				
		10	**20**	**30**	**40**	**50**
5	FE-RPT	7.8175	9.0331	9.7223	10.1756	10.5020
	FE-CPT	10.1395	13.3585	15.9409	18.1599	20.1360
	RPT [29]	7.8304	9.0458	9.7339	10.1864	10.5121
10	FE-RPT	9.5403	11.906	13.5305	14.7443	15.6957
	FE-CPT	10.3827	13.6789	16.3233	18.5955	20.6190
	RPT [29]	9.5628	11.9334	13.5598	14.7744	15.7267
20	FE-RPT	10.2079	13.2310	15.5414	17.4360	19.0484
	FE-CPT	10.4463	13.7627	16.4233	18.7094	20.7452
	RPT [29]	10.2349	13.2676	15.5845	17.4839	19.1002
50	FE-RPT	10.4246	13.6960	16.2967	18.5166	20.4757
	FE-CPT	10.4643	13.7864	16.4516	18.7417	20.7810
	RPT [29]	10.4530	13.7360	16.3474	18.5726	20.5377
100	FE-RPT	10.4569	13.7670	16.4169	18.6891	20.7082
	FE-CPT	10.4669	13.7898	16.4556	18.7463	20.7861

with orthotropy ratios 10 and 50 have been studied in Figures 8 and 9, respectively. By increasing the side-to-thickness ratio, the normalized frequencies increase firstly and then reach constant values. Figures 8 and 9 show that plates with stiffer boundary conditions possess higher normalized frequencies than the plates with softer boundary conditions. In Figures 10 and 11, the effects of orthotropy ratio (E_1/E_2) on normalized natural frequencies of thick ($a/h = 5$) and thin ($a/h = 100$) orthotropic plates are studied. By increasing the orthotropy ratio, the normalized frequencies increase and this ratio has more significant effect on normalized frequencies for thinner plates.

Table 10. Comparison of normalized natural frequency of FS plate.

a/h		E_1/E_2				
		10	**20**	**30**	**40**	**50**
5	FE-RPT	4.2797	4.8388	5.2589	5.5912	5.8629
	FE-CPT	4.9366	5.8489	6.6333	7.3334	7.9719
	RPT [29]	4.2840	4.8450	5.2661	5.5990	5.8710
10	FE-RPT	4.8152	5.6169	6.2744	6.8353	7.3251
	FE-CPT	5.0225	5.9517	6.7503	7.4630	8.1129
	RPT [29]	4.8210	5.6262	6.2861	6.8489	7.3401
20	FE-RPT	4.9890	5.8868	6.6483	7.3192	7.9233
	FE-CPT	5.0447	5.9783	6.7806	7.4965	8.1493
	RPT [29]	4.9954	5.8973	6.6621	7.3356	7.9419
50	FE-RPT	5.0418	5.9707	6.7672	7.4764	8.1217
	FE-CPT	5.0510	5.9857	6.7891	7.5059	8.1596
	RPT [29]	5.0483	5.9816	6.7816	7.4938	8.1417
100	FE-RPT	5.0496	5.9830	6.7848	7.4998	8.1515
	FE-CPT	5.0519	5.9868	6.7903	7.5073	8.1611

Table 11. Comparison of normalized natural frequency of FF plate.

a/h		E_1/E_2				
		10	**20**	**30**	**40**	**50**
5	FE-RPT	3.2575	3.2580	3.2585	3.2588	3.2591
	FE-CPT	3.5368	3.5369	3.5370	3.5372	3.5373
	RPT [29]	3.2577	3.2582	3.2586	3.2589	3.2591
10	FE-RPT	3.5100	3.5104	3.5107	3.5109	3.5110
	FE-CPT	3.5922	3.5104	3.5927	3.5929	3.5930
	RPT [29]	3.5102	3.5105	3.5108	3.5110	3.5111
20	FE-RPT	3.5849	3.5853	3.5856	3.5858	3.5859
	FE-CPT	3.6065	3.6068	3.6071	3.6072	3.6074
	RPT [29]	3.5851	3.5854	3.5857	3.5858	3.5859
50	FE-RPT	3.6070	3.6073	3.6076	3.6078	3.6079
	FE-CPT	3.6105	3.6108	3.6111	3.6113	3.6114
	RPT [29]	3.6072	3.6074	3.6077	3.6079	3.6080
100	FE-RPT	3.6102	3.6105	3.6108	3.6110	3.6111
	FE-CPT	3.6111	3.6114	3.6117	3.6119	3.6120

4. Conclusions

The finite element formulation for free vibration analysis of isotropic and orthotropic plates has been developed based on two-variable refined plate theory. This theory, which can be used for both thin and thick plates, predicts parabolic variation of transverse shear stresses across the plate thickness, satisfies the zero traction condition on the plate surfaces, and does not need the shear correction factor. After constructing weak-form equations using the Hamilton principle, a new 4-node rectangular plate element with six degrees of freedom at each node was introduced for discretization of the domains. The efficiency and accuracy of the presented formulation were proved by solving some benchmark isotropic and

Table 12. Comparison of normalized natural frequency of FF plate.

a/h		E_1/E_2				
		10	**20**	**30**	**40**	**50**
5	FE-RPT	2.5757	2.5750	2.5748	2.5748	2.5747
	FE-CPT	2.5048	2.8038	2.8036	2.8035	2.8035
	RPT [29]	2.5756	2.5749	2.5748	2.5747	2.5747
10	FE-RPT	2.7723	2.7714	2.7712	2.7711	2.7711
	FE-CPT	2.8389	2.8379	2.8387	2.8376	2.8376
	RPT [29]	2.7721	2.7713	2.7712	2.7711	2.7711
20	FE-RPT	2.8302	2.8293	2.8291	2.8290	2.8289
	FE-CPT	2.8476	2.8466	2.8464	2.8463	2.8463
	RPT [29]	2.8301	2.8292	2.8290	2.8289	2.8289
50	FE-RPT	2.8472	2.8463	2.8291	2.846	2.8459
	FE-CPT	2.8501	2.8491	2.8464	2.8488	2.8487
	RPT [29]	2.8470	2.8462	2.8460	2.8459	2.8459
100	FE-RPT	2.8497	2.8487	2.8485	2.8484	2.8484
	FE-CPT	2.8504	2.8494	2.8491	2.8491	2.8491

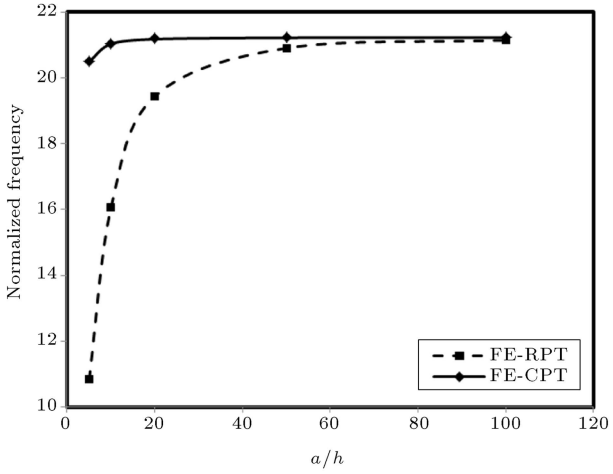

Figure 7. The effect of side-to-thickness ratio on normalized frequency of CC orthotropic plate ($E_1/E_2 = 10$).

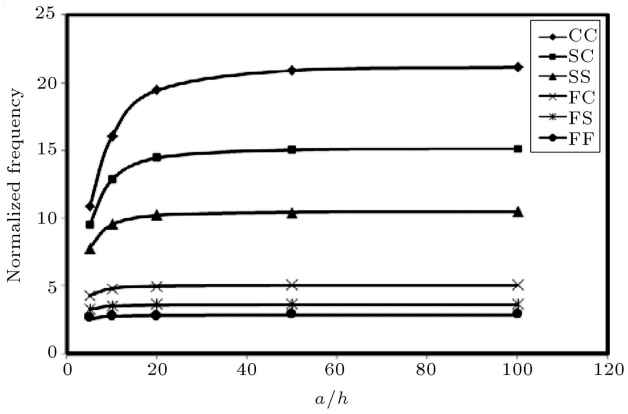

Figure 8. The effect of side-to-thickness ratio on normalized natural frequency of orthotropic plate ($E_1/E_2 = 10$).

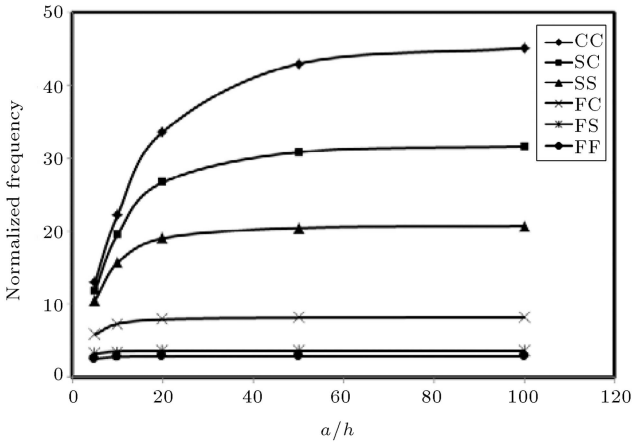

Figure 9. The effect of side-to-thickness ratio on normalized natural frequency of orthotropic plate ($E_1/E_2 = 50$).

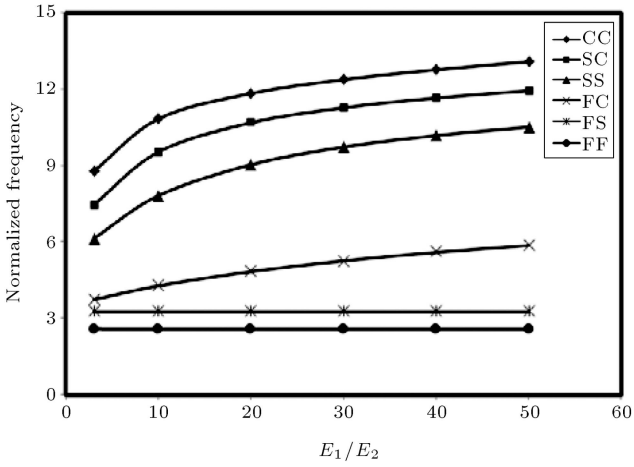

Figure 10. The effect of orthotropy ratio on normalized natural frequency of thick orthotropic plate ($a/h = 5$).

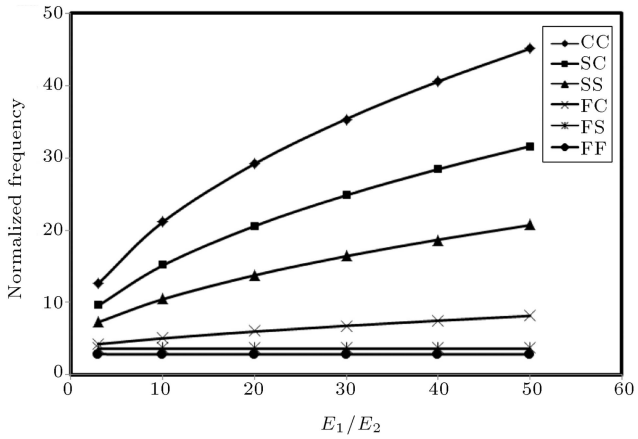

Figure 11. The effect of orthotropy ratio on normalized natural frequency of thin orthotropic plate ($a/h = 100$).

orthotropic plate problems. The comparison showed that besides simplicity of the presented formulation, the obtained results were in good agreement with exact values and analytical solutions available in the literatures. Because of considering shear deformation effects, the present formulation gave proper results for all natural frequencies of both thin and thick plates. By decreasing side-to-thickness ratio, the obtained frequencies converged to CPT results, which showed that the present formulation was free from shear locking effect. Also, the effects of side-to-thickness ratio, material properties, and types of boundary conditions on the obtained results were investigated.

References

1. Reissner, E. "The effect of transverse shear deformation on the bending of elastic plates", *J. Appl. Mech.*, **12**(2), pp. 69-77 (1945).
2. Mindlin, R.D. "Influence of rotary inertia and shear on flexural motions of isotropic elastic plates", *J. Appl. Mech.*, **18**(1), pp. 31-8 (1951).
3. Whitney, J.M. and Sun, C.T. "A higher order theory for extensional motion of laminated composites", *J. Sound Vib.*, **30**(1), pp. 85-97 (1973).
4. Hanna, N.F. and Leissa, A.W. "A higher order shear deformation theory for the vibration of thick plates", *J. Sound Vib.*, **170**(4), pp. 545-555 (1994).
5. Reddy, J.N. "A simple higher-order theory for laminated composite plates", *ASME. J. Appl. Mech.*, **51**(4), pp. 745-752 (1984).
6. Bhimaraddi, A. and Stevens, L.K. "A higher order theory for free vibration of orthotropic, homogeneous, and laminated rectangular plates", *J. Appl. Mech.*, **51**(1), pp. 195-198 (1984).
7. Kant, T. "Numerical analysis of thick plates", *Comput. Methods Appl. Mech. Eng.*, **31**(1), pp. 1-18 (1982).
8. Lo, K.H., Christensen, R.M. and Wu, E.M. "A high-order theory of plate deformation. Part 1: Homogeneous plates", *J. Appl. Mech.*, **44**(4), pp. 663-668 (1977).
9. Ghugal, Y.M. and Sayyad, A.S. "A static flexure of thick isotropic plates using trigonometric shear deformation theory", *J. Solid. Mech.*, **2**(1), pp. 79-90 (2010).
10. El Meiche, N., Tounsi, A., Ziane, N., Mechab, I. and AddaBedia, E.A. "A new hyperbolic shear deformation theory for buckling and vibration of functionally graded sandwich plate", *Int. J. Mech. Sci.*, **53**(4), pp. 237-47 (2011).
11. Shimpi, R.P. "Refined plate theory and its variants", *AIAA J.*, **40**(1), pp. 137-146 (2002).
12. Shimpi, R.P. and Patel, H.G. "A two variable refined plate theory for orthotropic plate analysis", *Int. J. Solids Struct.*, **43**(22), pp. 6783-6799 (2006).
13. Thai, H.T. and Kim, S.E. "Analytical solution of a two variable refined plate theory for bending analysis of orthotropic Levy-type plates", *Int. J. Mech. Sci.*, **54**(1), pp. 269-276 (2012).
14. Kim, S.E., Thai, H.T. and Lee, J. "A two variable refined plate theory for laminated composite plates", *Compos. Struct.*, **89**(2), pp. 197-205 (2009).
15. Shimpi, R.P. and Patel, H.G. "Free vibrations of plate using two variable refined plate theory", *J. Sound Vib.*, **296**(4-5), pp. 979-999 (2006).
16. Kim, S.E., Thai, H.T. and Lee, J. "Buckling analysis of plates using the two variable refined plate theory", *Thin Wall. Struct.*, **47**(4), pp. 455-462 (2009).
17. Thai, H.T. and Kim, S.E. "Levy-type solution for buckling analysis of orthotropic plates based on two variable refined plate theory", *Compos. Struct.*, **93**(7), pp. 1738-1746 (2011).
18. Narendar, S. "Buckling analysis of micro-/nano-scale plates based on two-variable refined plate theory incorporating nonlocal scale effects", *Compos. Struct.*, **93**(12), pp. 3093-3103 (2011).
19. Malekzadeh, P. and Shojaee, M. "Free vibration of nanoplates based on a nonlocal two-variable refined plate theory", *Compos. Struct.*, **95**, pp. 443-452 (2013).
20. Bhat, R.P. "Natural frequencies of rectangular plates using characteristic polynomials in Raliegh-Ritz method", *J. Sound Vib.*, **102**(4), pp. 493-499 (1985).
21. Misra, R.K. "Free vibration analysis of isotropic plate using multi-quadratic radial basis function", *Int. J. Sci. Env. Tech.*, **2**, pp. 99-107 (2012).
22. Semnani, S.J., Attarnejad, R. and Firouzjaei, R.K. "Free vibration analysis of variable thickness thin plates by two dimensional differential transform method", *ActaMechanica.*, **224**(8), pp. 1643-1658 (2013).
23. Liew, K.M., Huang, Y.Q. and Reddy, J.N. "Vibration

analysis of symmetrically laminated plates based on FSDT using the moving least squares differential quadrature method", *Comput Method Appl M.*, **192**(19), pp. 2203-2222 (2003)

24. Rouzegar, J. and Abdoli Sharifpoor, R. "A finite element formulation for bending analysis of isotropic and orthotropic plates based on two-variable refined plate theory", *Sci Iran- Tran. B: Mech. Eng.*, **22**(1), pp. 196-207 (2015).

25. Melosh, R.J. "Structural analysis of solids", *J. Struct. Div. ASCE*, **89**(4), pp. 205-223 (1963).

26. Hinton, E., *Numerical Methods and Software for Dynamic Analysis of Plates and Shells*, Swensea: Pineridge Press (1988).

27. Reddy, J.N. and Phan, N.D. "Stability and vibration of isotropic, orthotropic and laminated plates according to a higher-order shear deformation theory", *J. Sound Vib.*, **98**(2), pp. 157-170 (1985).

28. Liew, K.M., Wang, J., Ng, T.Y. and Tan, M.J. "Free vibration and buckling analyses of shear deformable plates based on FSDT mesh free method", *J. Sound Vib.*, **276**(3-5), pp. 997-1017 (2004).

29. Thai, H.T. and Kim, S.E. "Levy-type solution for free vibration analysis of orthotropic plates based on two variable refined plate theory", *Appl. Math. Model.*, **36**(8), pp. 3870-3882 (2012).

Biographies

Jafar Rouzegar is currently an Assistant Professor in the Department of Mechanical and Aerospace Engineering at Shiraz University of Technology, Iran. He received his BSc degree in Mechanical Engineering from Shiraz University, Iran, in 2002. He also received his MSc and PhD degree in Mechanical Engineering from Tarbiat Modares University, Iran, in 2004 and 2010, respectively. His research interests include: FEM and XFEM, fracture mechanics, and theories of plates and shells.

Reza Abdoli Sharifpoor received his BSc degree in Mechanical Engineering from Bu Ali Sina University, Hamedan, Iran, in 2011. He also received his MSc degree in Mechanical Engineering from Shiraz University of Technology, Iran, in 2014. His research interests include FEM, theories of plates and shells, and composite materials.